CHAPTER II
BACKGROUND AND LITERATURE SURVEY

2.1 Theoretical Background

For a vertical pipe, there are four main regimes, as shown in Figure 2.1 and 2.2, occurring successively at ever-increasing gas flow rates:

(a) *Bubble Flow*: There is a continuous liquid and the gas phase dispersed as bubble within the liquid continuum. The bubbles travel with complex motion causing the bubbles coalescing and generally are of non-uniform size.

(b) *Slug Flow*: This flow pattern, which, in vertical systems, is sometimes referred to as plug flow, occurs when the bubble size tends toward that of the channel diameter, and characteristic bullet-shaped bubbles are formed. A bubble surrounded by liquid thin film is often called a Taylor bubble. The liquid between the Taylor bubbles often contains a dispersion of smaller bubbles.

(c) *Churn Flow*: At higher gas velocities, the Taylor bubbles in slug flow break down into an unstable pattern in which there is a churning or oscillatory motion of liquid. This flow occurs more predominantly in wide-bore tubes and may not be so important in narrow-bore tubes where the region of churn flow is small.

(d) *Annular Flow*: This configuration is characterized by the liquid phase travelling as a film on the channel walls, and the gas phase flowing through the center. Part of the liquid can be carried as droplets in the central gas core.

(e) *Mist Flow*: The velocity of the continuous gas phase is so high that it reaches as far as the tube wall and entrains the liquid in the form of droplets.

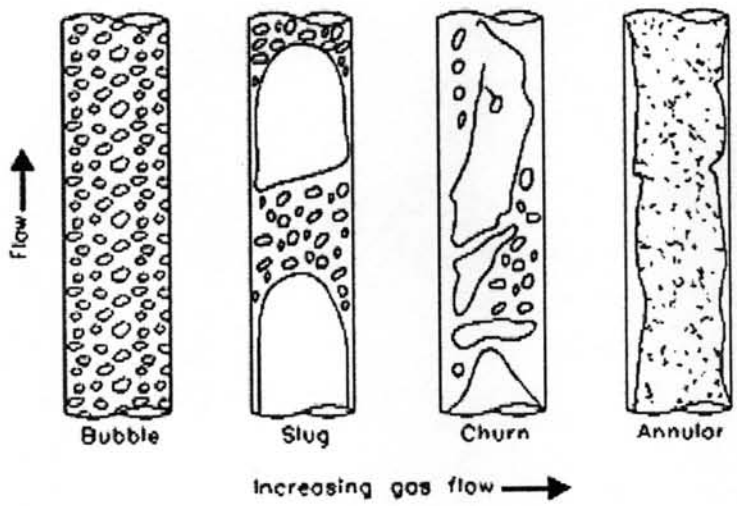

Figure 2.1 Modelling flow pattern transitions for steady Upward Gas-liquid Flow in Vertical Tubes (Bornea, and Dukler, 1980).

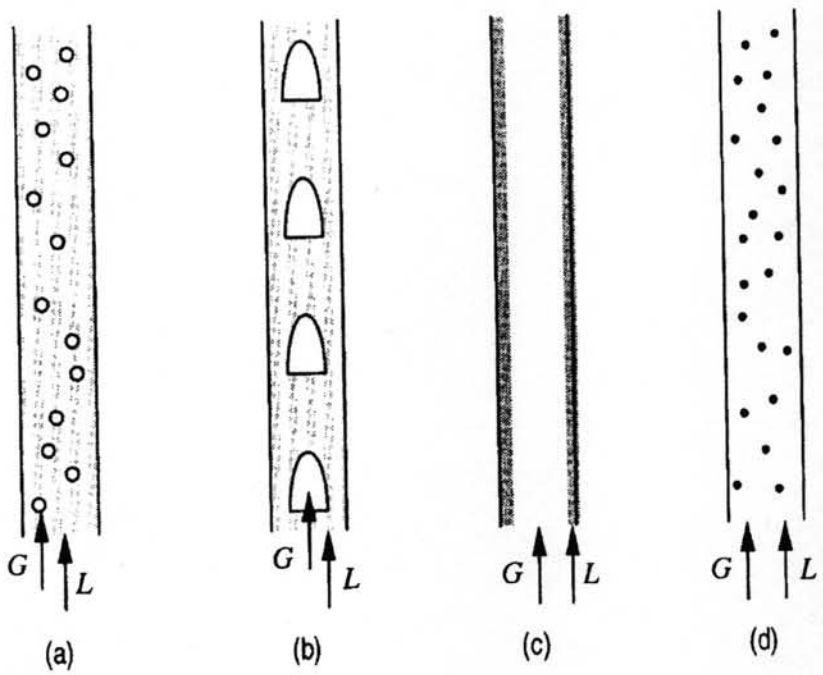

Figure 2.2 Two-phase flow regimes in a vertical tube: (a) bubble; (b) slug; (c) annular; and (d) mist flow. In each case, the gas is shown in white, and the liquid is shaded in black (Wilkes, 1999).

2.1.1 Determination of Flow Regime

A typical situation occurs when the gas and liquid volumetric flow rates G and L are specified, and the pressure gradient *dp/dz* and void fraction are calculated. Correlations for these last two variables are more likely to be successful if we can recognize the particular flow regime and develop relationships specifically for it. The following approximate demarcations are recognized:

2.1.1.1 Bubble/ Slug Flow Transition.

Small bubbles introduced at the base of a column of liquid will usually and eventually coalesce into slugs. The transition depends very much on the size of the bubbles, how they are introduced, the distance from the inlet, and on surface tension effects, so there is no simple criterion for the transition.

2.1.1.2 Slug/ Annular Flow Transition.

In the narrow gap between the gas and the tube wall at the base of the slugs, there is a significant downwards flow of liquids, and hence a fairly strong relative velocity between gas and liquid in the point. For increasing gas flow rates, the result is instability of the liquid film, which can start bridging the whole cross section of the tube. These bridges can in turn be broken up by the gas and the flow becomes chaotic.

2.1.1.3 Annular/ Mist Flow Transition.

The transition is ill-defined because most annular flow entrains some droplets.

2.1.2 Bubble Flow Regime

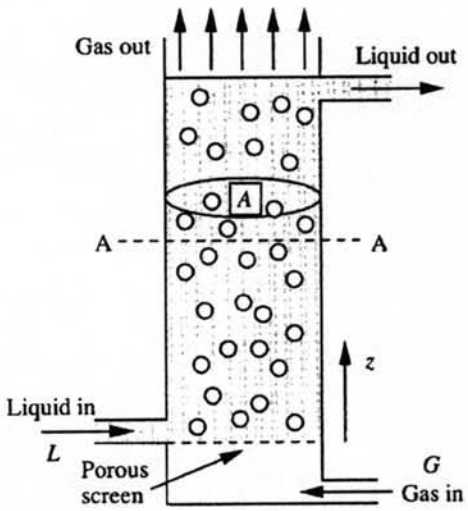

Figure 2.3 Bubble flow (Wilkes, 1999).

Gas bubbles and liquid in upward co-current flow are shown in Figure 2.3. The mean upward liquid velocity across plane A-A is

$$\bar{u}_l = \frac{G + L}{A} \tag{2.1}$$

where, G = Volumetric flow-rate of gas, ccm

L = Volumetric flow-rate of liquid, ccm

A = Cross-sectional area of a tube, cm^2

The rise velocity of gas bubbles below plane A-A are relative to a moving liquid which has a velocity ($\bar{u}_l$), so that velocity of the gas bubbles is:

$$v_g = \bar{u}_l + u_b = \frac{G + L}{A} + u_b \tag{2.2}$$

where u_b is the bubble velocity rising into a stagnant liquid. The bubble velocity, u_b rising into a stagnant liquid was proposed by Peebles and Garber (1953).

$$\text{Bubble velocity} = u_b = 1.00\sqrt{g\,R_b} \tag{2.3}$$

where g = gravitational acceleration constant (m/s^2), R_b = radius of sphere that has the same volume as the spherical-cap bubble (m) and total volumetric flow rate of gas is:

$$G = \varepsilon A v_g \tag{2.4}$$

So, the void fraction is given by:

$$\frac{G}{\varepsilon A} = \frac{G+L}{A} + u_b \qquad \text{or} \qquad \varepsilon = \frac{G}{G+L+u_b A} \tag{2.5}$$

The pressure gradient is given fairly accurately by considering only the hydrostatic effect. For the relatively low liquid velocities likely to be encountered in the bubble-flow regime, friction is negligible.

$$\frac{dp}{dz} = -\rho_l g(1-\varepsilon) \tag{2.6}$$

2.1.3 Slug Flow Regime

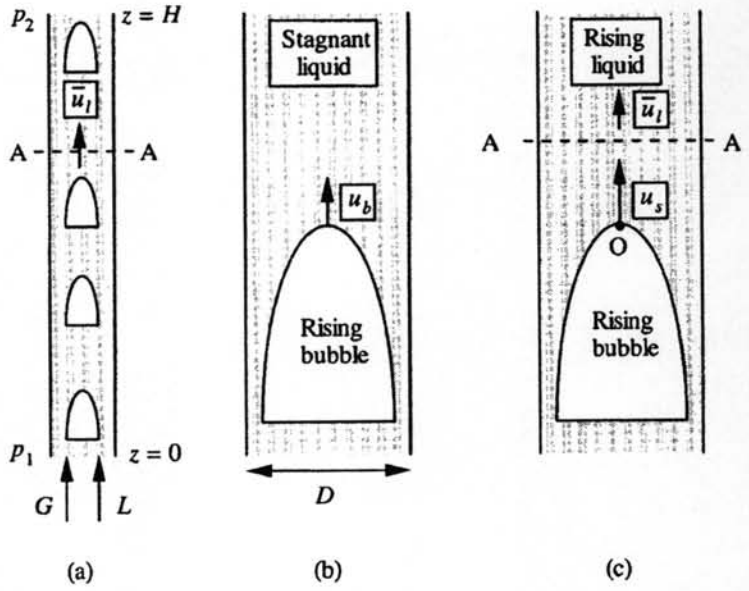

Figure 2.4 Two-phase slug flow in a vertical pipe: (a) ascending gas and liquid; (b) rising bubble in stagnant liquid; (c) rising bubble in moving liquid (Wilkes, 1999).

Figure 2.4(a) shows the gas and liquid flow upwards together at single volumetric flow rates G and L, in a pipe of internal diameter D. An upwards liquid velocity (u_l) across a plane A-A is leading of a gas slug. The total upward volumetric flow rate of liquid across A-A must be the combined gas and liquid flow rates which enter at the bottom. Therefore the mean liquid velocity at plane A-A is $\bar{u}_l = (G+L)/A$, in which A is the cross-sectional area of the pipe.

Figure 2.4(b) shows a different situation that of a single bubble is moving steadily upward with a rise velocity u_b in a stagnant liquid. Davies and Taylor (1950) used an approximate analytical solution for the non viscous liquid such as water and light oils, which is

$$u_b = c\sqrt{gD} \tag{27}$$

where the constant c = 0.33 and g is the gravitational acceleration. From the experimental data (The mechanics of large bubbles rising though extended liquids and though liquid in tubes), the constant c should equal to 0.35.

A slug rises in a stagnant liquid, as shown in Figure 2.4(b) and the highest velocity occurs at the center of the pipe-near the nose of the slug. Nicklin, Wilkes, and Davision (1962), showed that the value of liquid velocity of was about $1.2\bar{u}_l$, when the Reynolds numbers were greater than 8,000.

Hence, the true rise velocity of the slug is:

$$u_s = 1.2\frac{G+L}{A} + u_b = 1.2\frac{G+L}{A} + 0.35\sqrt{gD} \tag{2.8}$$

From the conservation of the gas; this gives:

$$G = u_s A\varepsilon \tag{2.9}$$

Substituting u_s in equation (2.9) to (2.8)

$$\frac{G}{\varepsilon A} = 1.2\frac{G+L}{A} + 0.35\sqrt{gD} \tag{2.10}$$

The equation (2.10) can be solved for the void fraction when the gas and liquid flow rates are known. It is very important to determine the pressure drop in a tube of height H. Also note that the weight of the liquid, which occupies a fraction (1-ε) of the total volume, is much greater than that of the gas. Therefore, the pressure drop is given to a first approximation by

$$p_1 - p_2 = \rho_L g H(1-\varepsilon) \tag{2.11}$$

A secondary correction to equation (2.11) would include the wall friction on the liquid "pistons" between successive gas slugs. Thus, if $(dp/dz)_{sp}$ is single-phase frictional pressure gradient for liquid only, flowing at a mean velocity $\bar{u}_l$, a more accurate expression for the pressure gradient is

$$\frac{dp}{dz} = (1-\varepsilon)\left[-\rho_l g + \left(\frac{dp}{dz}\right)_{sp}\right] \tag{2.12}$$

Sylvester (1987) showed the mechanistic model for calculating pressure gradient for slug flow. The mechanistic model for vertical slug flow is formulated based on the assumption that the flow is fully developed and stable. This assumption requires that the liquid slug and the Taylor bubble rise steadily without any relative velocity between them. The model is developed for a slug unit consisting of one Taylor bubble with its surrounding liquid and one liquid slug. The idealized slug unit is shown in Figure 2.5.

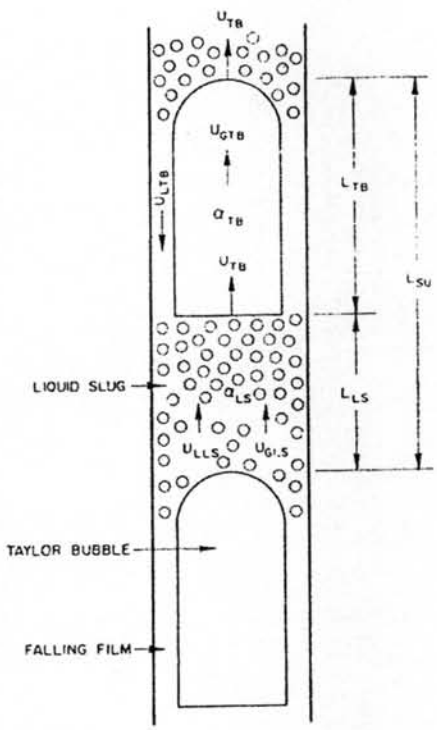

Figure 2.5 Slug unit (Sylvester, 1987).

Table 2.1 Model variables for Sylvester theory

L_{SU}	Length of the slug unit (m)
L_{TB}	Length of the Taylor bubble (m)
L_{LS}	Length of the liquid slug (m)
α_{TB}	Void fraction of the Taylor bubble
α_{LS}	Void fraction of the liquid slug
α_{SU}	Void fraction of the slug unit
U_{TB}	Velocity of the Taylor bubble (m/s)
U_{LTB}	Velocity of the liquid film around the Taylor bubble (m/s)
U_{GTB}	Velocity of the gas in Taylor bubble (m/s)
U_{GLS}	Velocity of the gas in liquid slug (m/s)
U_{LLS}	Velocity of the liquid in the liquid slug (m/s)

The large gas bubbles or Taylor bubbles occupy nearly the entire pipe cross section and translate steadily upward with a velocity, U_{TB}. For fully developed slug flows of low viscosity liquids, the ideal Taylor bubbles are long cylindrical voids having a spherical nose and a flat tail. Their length L_{TB} will remain constant in the axial direction provided expansion effects are negligible. The liquid film flows past the Taylor bubble with velocity, U_{LTB}. The Taylor bubble is followed by a liquid slug which contains numerous small gas bubbles. It is assumed that these small bubbles are distributed uniformly throughout the liquid slug with a void fraction given by α_{LS}. The length of the liquid slug, L_{LS}, also remains constant.

Stable slug flow is visualized to be continuous train slug units which move steadily upward along the pipe at a velocity U_{TB}. Although this is an idealized picture of vertical slug flow, it represents a fairly accurate model of the actual situation from a time-averaged point-of-view.

The total pressure drop in the slug unit consists of three components

$$(\Delta P)_T = (\Delta P)_A + (\Delta P)_H + (\Delta P)_F \qquad (2.13)$$

where

$(\Delta P)_T$ is total pressure drop in the slug unit (Pa)

$(\Delta P)_A$ is acceleration pressure drop (Pa)

$(\Delta P)_H$ is hydrostatic pressure drop (Pa)

$(\Delta P)_F$ is frictional pressure drop (Pa)

The acceleration pressure drop is taken to be that required to reverse the direction and accelerate the liquid film falling around the Taylor bubble to the velocity U_{LLS}. This pressure drop can be written as

$$(\Delta P)_A = \rho_L(U_{LTB} + U_{TB})(1-\alpha_{TB})(U_{LTB} + U_{TB} + U_{LLS}) \tag{2.14}$$

where

$$U_{LTB} = 9.916\left[gD\left(1-\sqrt{\alpha_{TB}}\right)\right]^{1/2} \tag{2.15}$$

$$U_{TB} = 1.2(U_{SG} + U_{SL}) + 0.35\left[\frac{gD(\rho_L - \rho_G)}{\rho_L}\right]^{1/2} \tag{2.16}$$

The hydrostatic pressure drop of the slug unit can be written in the form

$$(\Delta P)_H = \rho_L(1-\alpha_{LS})gL_{LS} \tag{2.17}$$

where

$$\alpha_{LS} = \frac{U_{SG}}{C_2 + C_3(U_{SG} + U_{SL})} \tag{2.18}$$

Thus equation (2.18) with $C_2 = 0.425$ and $C_3 = 2.65$ is chosen. It must be emphasized that although the form of equation (2.18) is theoretically sound, the coefficient were determined from a best least squares fit of Fernandes experiment data.

The frictional pressure drop of slug unit can be written as

$$(\Delta P)_F = \frac{L_{LS}}{2D}\left[\frac{\rho_G \beta f_{TB} U_{TB}^2}{(1-\beta)\left[1-(1-\alpha_{TB}^{1/2}\right]} + U_{LLS}^2 \rho_L (1-\alpha_{LS}) f_{LS} (1-\beta)\right] \tag{2.19}$$

where

$$\beta = L_{TB}/L_{SU} \tag{2.20}$$

f_{TB} is friction factor associated with the Taylor bubble. If it is assumed that the falling rough surface to the Taylor bubble, the Taylor bubble friction factor mat be written as

$$f_{TB} = \frac{1}{\left[-2.0\log\left\{\frac{\left(1-\alpha_{TB}^{1/2}\right)}{7.4}\right\}\right]^2} \tag{2.21}$$

f_{LS} is the friction factor associated with the liquid slug which in general depends upon the Reynolds number of the liquid slug , Re_{LS}, and the pipe roughness. This dependency can be expressed as

$$f_{LS} = f_{LS}\left(\mathrm{Re}_{LS}, \varepsilon / D\right) \tag{2.22}$$

where ε is the pipe roughness, and

$$\mathrm{Re}_{LS} = \frac{\rho_L\left(1-\alpha_{LS}\right)U_{LLS}D}{\mu_{LS}} \tag{2.23}$$

Since $\mu_L >> \mu_G$ equation (2.23) may be simplified to

$$\mu_{LS} \cong \mu_L\left(1-\alpha_{LS}\right) \tag{2.24}$$

Equation (2.22) can be expressed explicitly using the Zigrang-Sylvester equation which is an explicit which is an explicit representation of the Colebrook equation.

$$f_{LS} = \frac{1}{\left[-2.0\log\left\{\frac{\varepsilon/D}{3.7} - \left(\frac{5.02}{\mathrm{Re}_{LS}}\right)\log\left(\frac{\varepsilon/D}{3.7} + \frac{13}{\mathrm{Re}_{LS}}\right)\right\}\right]^2} \tag{2.25}$$

Substituting equation (2.14), (2.17) and (2.19) into equation (2.13) gives the total pressure drop for slug unit.

$$(\Delta P)_T = \rho_L (U_{LTB} + U_{TB})(1-\alpha_{TB})(U_{LTB} + U_{TB} + U_{LLS}) + \rho_L (1-\alpha_{LS}) g L_{LS}$$

$$+ \frac{L_{LS}}{2D}\left[\frac{\rho_G \beta f_{TB} U_{TB}^2}{(1-\beta)\left[1-(1-\alpha_{TB}^{1/2}\right]} + U_{LLS}^2 \rho_L (1-\alpha_{LS}) f_{LS} (1-\beta)\right] \qquad (2.26)$$

2.1.4 Churn or Froth Flow Regime

The froth flow pattern has been variously called churn, froth, wave entrainment, dispersed plug, and semi-annular. It is similar to the slug pattern in that the flow is pulsating and there are alternate slugs of gas and liquid. At the higher flow rates characteristic of froth flow, the bubble wakes become more agitated, a large number of small bubbles are torn off at the tail, and the whole wake becomes richer in bubbles. The froth pattern differs from the regular orderly slug flow pattern in that neither the bubbles of gas nor the slug of liquid maintain their identity as they moved up the tube.

The pattern occurs over a modest range of superficial gas velocities and apparently only up to a certain critical superficial liquid velocity. It is a transition pattern from the regular slug flow to the annular-mist flow. At any given liquid rate, the pattern extends from the point of breakdown of the regular liquid slugs and gas bubbles to a gas velocity sufficient to carry the bulk of the liquid up the wall of the tube by the surface drag exerted.

The froth flow pattern is not amenable to theoretical analysis and has not been the subject of any extensive experimental study.

2.1.5 Annular-Mist Flow Regime

The annular-mist flow pattern is widely encountered in the flow of gas-liquid mixtures at high gas rates and gas-liquid ratios. The annular-mist flow pattern in gas-liquid systems is characterized by an upward moving, continuous, and smooth to wavy film of liquid on the tube wall and a much more rapidly moving central core of gas, containing entrained droplets of liquid in a concentration which

may vary from low to high. The liquid film may be wholly in laminar motion or it may be laminar only nearest the wall, and turbulent nearest the gas-liquid interface.

Shearer and Nedderman (1965) divided the annular-mist flow pattern into the "small ripple" regime and the "disturbance wave" regime. In the small ripple regime, small waves develop on the liquid surface and move at velocities of the order of the interface velocities and then lose their identity. At higher liquid flow rates, the waves are larger, and they travel at velocities two to five times the interfacial velocity. These waves are known as disturbance waves.

At any given liquid rate, decreasing the gas rate causes more of the liquid to be present in the film, the liquid film velocity to decrease, and its thickness to increase. At a certain critical gas rate, the liquid film velocity becomes zero, and below this rate the liquid film has a negative velocity near the wall, and it penetrates the gas phase, and the froth flow occurs. As the gas rate is increased, turbulence takes place in the liquid film, the thickness of the film decreases, waves develop at the interface, and an increasing number of droplets are torn from the film and entrained in the gas. Eventually the continuous film is destroyed and almost all the liquid is transported as entrained droplets in the gas phase.

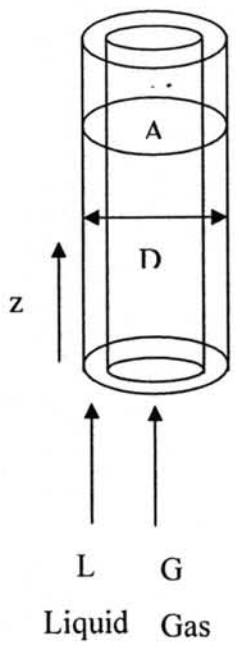

Figure 2.6 Vertical annular two-phase flow (Wilkes, 1999).

The simultaneous flow of gas and liquid in a vertical tube as shown in Figure 2.6. First, consider just the flow of gas in the inner core. Since the gas velocity v_g is typically much higher than that of the liquid, the pressure gradient may be approximated as if the gas were flowing with velocity v_g in a pipe of diameter D_g, giving:

$$\left(\frac{dp}{dz}\right)_{tp} = \left(\frac{dp}{dz}\right)_g = -\frac{2f_F\,\rho_g\,v_g^2}{D_g} - \rho_g g = \phi_g^2\left(\frac{dp}{dz}\right)_{go} - \rho_g g \quad (2.27)$$

Second, consider the entire flow, obtaining the frictional contribution from the viewpoint of the liquid:

$$\left(\frac{dp}{dz}\right)_{tp} = \phi_l^2\left(\frac{dp}{dz}\right)_{lo} - \left[\varepsilon\,\rho_g + (1-\varepsilon)\,\rho_l\right]g \quad (2.28)$$

For specified gas and liquid flow rates, the derivatives on the right-hand sides of both equations will be known by calculation. These equation can then be solved simultaneously for the two-phase flow pressure gradient $(dp/dz)_{tp}$ and the void friction ε.

2.2 Literature Survey

Lockhart and Martinelli (1949) presented the simultaneous flow of air and liquid including kerosene water and various oils in pipes by varying in diameter. Four types of isothermal two-phase, two-component flow were shown to exist depending upon whether each phase was viscous or turbulent. They concluded that the static pressure drop for the liquid phase was quite equal to the static pressure drop for the gas phase regardless of the flow pattern, as long as an appreciable radial static pressure difference did exist. The volume occupied by the liquid plus the volume occupied by the gas at any instant were equal to the total volume of pipe. They postulated that the flow pattern did not change along the tube length.

Nicklin (1962) analyzed the motion of the bubbles in two phase flow. A theory was presented which shows that the velocity of the bubbles consisted of a component equal to superficial liquid velocity, a component equal to the superficial gas velocity and a component due to buoyancy. He found that the motion of bubble in two phase bubble flow a raised partly from buoyancy and partly from the superficial velocity caused by the entry of the two phases in to the tube. The energy loss due to slip was closely related to the buoyancy component of rising velocity.

Sylvester (1987) presented the formulation of a mechanistic model for slug flow in vertical pipes. The equation required determining hold up, the relevant velocities and pressure losses were presented. The model was fully deterministic and the pressure drop predictions of the model were compared to experiment field data for oil and gas and water wells. He found that slug flow was predicted to occur in 82 of the 83 cases and the model predicts the pressure drops different from the experiment about 4.83 percent

Fukano and Kariyasaki (1993) examined the characteristic of an air-water isothermal two-phase flow in capillary tube with the inner diameter of 1 mm, 2.4 mm, 4.9 mm and 9 mm. The directions of flow were vertical upward, horizontal and vertical downward. They found that capillary force becomes important in the case that the tube inner diameter is less than 5 mm-9 mm. Flow pattern did not change a great deal according to flow direction, even in the horizontal flow the flow pattern became symmetrical, and the water film thickness was circumferentially uniform. Small bubbles usually do not exist in liquid slug and liquid films.

Cachard and Delhaye (1996) proposed about airlift pumping process, air was injected into the pipe containing fluid to be transferred. Small diameter air lift pump was used for corrosive or radioactive liquids. The experiments included differential pressure and void fraction measurements. The air lift model proposed used a linear combination of models describing wall friction in slug and churn flow. There two models were based on the general literature on two phase flow. The steady state model proposed represented an accurate analysis tool for the design of small diameter (up to 40 mm), tall (length to diameter ratio greater than 250) airlifts. Not only the airlift overall performance was accurately predicted, but also the separate

contribution of the gravity and the friction term, as indicated by the detailed measurements performed.

Saroha and Khera (2006) investigated the two phase pressure drop across the tickle bed reactor. It is a crucial parameter in the design, scale-up and operation because it is a measure of the energy required in a moving the fluid through the reactor. Experiment were performed with air-water system using glass beads as packing material at ambient conditions of temperature and pressure for upflow and downflow mode of operation. They found that two-phase pressure drop increased with an increase in gas and liquid velocity. The upflow mode of operation provided a complete wetting and was advantageous when the reaction was exothermic as it prevented the formation of hot spots. But downflow mode of operation is the preferred mode of operation in the industry due to the relatively lower pressure drop in downflow mode of operation.

Costigan and Whalley (1997) studied the dynamic variation, of void fraction in air-water flow in a vertical 33 mm diameter tube; the data presented cover flow patterns from bubble to annular. They found that as gas flow was increased at constant liquid flow, Taylor bubble lengths increased but their void fractions fell. Slug lengths gradually decreased and their void fraction rose. As liquid velocity was increased at constant gas velocity, bubble lengths decreased with approximately constant void fractions. Slug lengths and void fractions tended to remain constant but the number of slugs and bubble increased at the same rate as the bubble length falls.

Cachard and Delhaye (1998) studied the detailed description of steady state flow in a small diameter airlift pump. They found that airlift instabilities were due to density wave's oscillations in the two phase flow section. Depending on the liquid flow inertia, friction terms and on the gas flow compressibility term. Their linear analysis performed predicted the complex and interacting effects of the geometrical parameter and the gas flow rate well. The stability prediction, for a given airlift operating point within the linear stability domain, was based on the first (lower) oscillatory frequency predicted by the linear analysis for this point. If this frequency is far enough from the equivalent frequency (first oscillatory mode) at the linear stability boundary, the point is predicted as stable.

King *et al.* (1998) studied the effect of flow rate transients within slug flow regime was carried out in the WASP facility. The test section consisted of a 36 m long, nominal 3-inch diameter stainless steel pipe. Air and water were used as the test fluids and determine the response to change flow rate. The results presented the slug flow regime cannot be modelled by a quasi-steady approach since some features of gas transients are not predicted by considering the flow as a succession of steady states. The foremost of these features was the overshoot in the inlet pressure in response to an increase in the gas velocity. Furthermore, the observed period of intense slugging is not a feature of steady state model. For the decreasing gas transient in which the flow became quiescent and the slug decay was promoted. The pressure undershooted below the new steady state pressure was caused by a decreased pressure drop along the test section.

Watson and Hewitt (1999) studied the effect of pressure on the slug/churn flow pattern transition in vertical upwards gas-liquid flow. The experiments were conducted with air-water flow in a 32 mm, 12.6 m long tube. They found that increasing the liquid flow rate increased the gas flow rate required to initiate the slug/churn transition, though the effect is small at the highest range of liquid flow rate covered. An increase in pressure decreased the superficial gas velocity at the transition.

Hawke *et al.* (2000) studied the characteristics of annular two phase flow at high mass fluxes and measured the pressure gradient fluctuation. The results presented the behaviour of core structures (wisps) in annular flow at high mass fluxes. The wisps appeared to have frequencies of the order of 5-8 Hz and to travel at velocities approaching that of the core. The core structures were a manifestation of instability of the highly concentrated gas-droplet mixture. A gamma densitometer which indicated the concentration was inaccurate because the resolution was inadequate.

Barbosa *et al.* (2001) his work has dealt with experiment and modelling on churn flow of an air-water mixture in a vertical pipe. High-speed video photography has been used to study the behaviour of the flow close to the liquid inlet in a specially constructed transparent porous-wall test section. They found that the process of wave formation in churn flow which, in this case was co-existing with a

falling film below the injector. The velocity and wave frequencies from the video recordings gave results which were broadly consistent with previous results of Hewitt et al. (1995). A simple model to describe the wave levitation process was unable to predict such a complex regime as churn flow because the model was calibrated against measurements of the location of the waves as a function of time.

Delfos *et al.* (2001) measured the gas loss from a Taylor bubble that was held stationary in a downward liquid flow and investigate void fraction in the downward bubbly flow below the Taylor bubble. From the experiment show that below the Taylor bubble base there was a strongly recirculation wake, with length of about 1-1.5 D, independent of the film entrance velocity or the film flow rate. The Taylor bubble hardly lost air below a curtain length which ranged from 0.3 m for turbulent to 0.5 m for laminar upstream flow. They founded a highly intermittent entrainment process, in which small clouds of bubbles were entrained from the Taylor bubble in to the wake. The gas loss from the Taylor bubble increased with increasing liquid flow rate.

Hajiloo *et al.* (2001) determined the friction in downward co-current two-phase flow for water and air flow Reynolds numbers in the ranges 5100-27200 and 3400-21600, the data was unique in that the tube diameter varied from 4.13 cm to 1.56 cm to demonstrate the critical importance of this parameter the experimental techniques ensured that organic surfactants were not present to affect the interfacial wave structure. They found that the friction coefficients were agreement with most previously reported data. At a fixed gas Reynolds number, a large increase in friction accompanied a decrease in tube diameter.

Barbosa *et al.* (2002) studied the droplet entrainment and the pressure gradient for the transition region between the churn flow and the annular flow in a vertical pipe (31.8 mm internal diameter, 10.8 m long). They found that in the co-current annular region ($U^*_{GS}>1$), the droplet concentration was virtually constant within the gas core. In contrast, in the region of transition between churn flow and annular flow the droplet concentration varied across the core. Both pressure gradient and entrained fraction exhibited a minimum at $U^*_{GS}=1$, before increasing again in the annular regime which droplets were created from interfacial waves present on a liquid film.

Mcneil *et al.* (2003) investigated the effects of a highly viscous liquid by using water and glycerine solution to produce liquid viscosities of 1, 50, 200 and 550 mPa s. These liquids flowed concurrently with air to allow measurements of momentum flux, void fraction and pressure distributions. The flow pattern in pipe was annular up-flow. They found that existing momentum flux and void fraction methods did not extend to the highly viscous range and that only the Chisholm C model has any success in representing the frictional pressure gradient. This study showed that for the annular flow regime and the interfacial friction factor can be found from the proposed correlation.

Carvalho (2006) studied the hydrodynamic behaviour of very long gas slugs of argon with densities in the range 6.6-21.5 kg/m^3, rising co-currently with water along a 20 mm inside diameter vertical tube. The video sequences of the process showed that the instability of the slugs was associated with flooding of the slug core by the liquid, which is dragged up by the gas. While the gas density and liquid velocity were raised above certain levels, they lost their integrity/identity at some distance down from the slug nose. For the lower gas densities liquid velocity the slugs were stable, but for higher liquid velocity and/or gas densities, the slugs would become unstable, as a result of flooding in the wetted wall flow around them.

Felipe (2006) presented a rational thermodynamic model which consistently incorporated internal surface tension effects in a homogeneous and isothermal two-component two phase flow. The model was capable to continuously emulate the internal surface tension effects in liquid-gas flows over the whole range of the void fraction without loosing the hyperbolic of the governing equations. For air-water mixture that internal surface tension affected the speed sound in a bubbly flow but did not affect it in a droplet one. The theoretical predictions of speed of sound calculated the classical model and the proposed model were compared with the experimental data for air-water systems. It was shown that the proposed model presented a better agreement than the classical one.